ARTICLES

Efficient Electrooptic Polymers for THz Applications†

Alexander M. Sinyukov and L. Michael Hayden*

Department of Physics, University of Maryland, Baltimore County, Baltimore, Maryland 21250

Received: September 4, 2003; In Final Form: December 31, 2003

We present a method for producing electrooptic (EO) polymer films with EO coefficients 40−50 pm/V at 785 nm which are suitable for use as emitters and sensors of THz radiation. Direct comparison with ZnTe shows that our EO polymers are more efficient THz emitters than ZnTe. The THz field generated from a 80 μm thick poled polymer film is equal to that generated from a 1 mm thick ZnTe crystal. A model for the THz generation via optical rectification from a poled polymer has been developed and verified experimentally in a THz system using a polymer emitter and a ZnTe sensor.

Introduction

During the last 10 years THz radiation has found many applications in industry and science, attracting high interest to this area. Because of their long wavelength (100−300 μm), THz waves propagate easily through nonpolar, nonmetallic material such as paper, card board and plastic. If an object is inserted in a THz beam, a THz image can be obtained. In contrast with X-rays, THz radiation is nonionizing. This advantage allows T-ray imaging to be a powerful diagnostic tool in medicine and biology.[1−3] T-ray imaging can be also used for food and package inspection and industrial quality control.[4,5] Other applications of THz waves include trace gas analysis, flame emissions,[6] impulse ranging,[7,8] and THz-interferometry.[9]

When a THz wave passes through an object, information about the object's dielectric properties can be obtained. This is the basis of THz time-domain spectroscopy (THz-TDS). By comparing changes in the amplitude and phase of the THz electric field of a signal pulse, recorded when the sample is in the THz beam path, and a reference pulse, obtained without the sample, detailed, frequency-dependent information about the absorption coefficient and refractive index of the material under study may be obtained.[10−14]

Sensitivity, signal-to-noise ratio, and frequency response are the factors of primary importance for all the THz applications above. These factors depend on the THz emitters and detectors used.

Among the many ways to emit and detect THz radiation already tested, coherent THz systems with photoconductive dipole antennas[11] and EO materials[15] as THz emitters and detectors are widely used today. EO materials include inorganic and organic crystals and EO polymers. While crystals (inorganic ZnTe[16] GaAs,[17] and GaP[18] and organic DAST[19] and MBANP[20]) are widely used in THz experiments, EO polymers have been comparatively less explored in this regard. Only a small number of papers using EO polymers have been published.[21−25]

The goal of this paper is to highlight the properties of EO polymers that make them attractive for THz applications. In addition, we make direct comparisons of the THz performance of our EO polymers and the most widely used crystal, ZnTe, which demonstrate that EO polymers are efficient and promising THz emitters and detectors due to their larger EO coefficients and longer coherence lengths.

This paper is organized as follows. First, we describe the materials we are working with and the THz experiment used to test these materials. Then, we present a model developed for a system of an EO polymer emitter and ZnTe detector. Experimental verification of this model and other THz results with EO polymers are then given. Finally, we compare the coherence length of crystals and our polymers. In the conclusion, we summarize our study and discuss future experiments.

Materials

We are working with guest−host polymer composites. They have two components, a guest chromophore and a polymer matrix host. Our chromophores possess large dipole moments (Figure 1), allowing easy orientation in an external electric field. Various polymer matrices like PMMA, polystyrene, polycarbonate, and APC (poly(bisphenol A carbonate-*co*-4,4′-(3,3,5-trimethylcyclohexylidene)diphenol carbonate)) can be used as hosts.

There is always a trade off between the concentration of the chromophore and the orientational stability of the EO composite. Increasing the amount of chromophore in the composite causes an increase of the EO coefficient (eq 1). This is a reason to increase the concentration of chromophores as much as possible until phase separation (or crystallization) is observed. On the other hand, increased chromophore concentration leads to a decrease of the glass transition temperature (T_g) of the composite because the chromophore acts as a plasticizer for the polymer host. Therefore, in general, the higher the initial T_g of the polymer host the higher will be the eventual T_g of the composite. In turn, the higher the T_g of the composite the more stable the polar order of the chromophores.

† Part of the special issue "Alvin L. Kwiram Festschrift".

* Corresponding author. E-mail: hayden@umbc.edu.

10.1021/jp036644l CCC: $27.50
Published on Web 05/05/2004

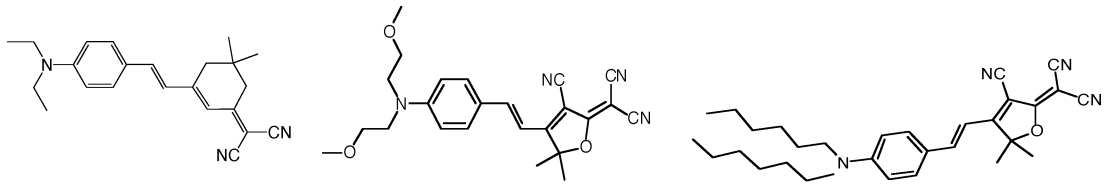

Figure 1. Chromophores and corresponding dipole moments μ and figures of merit (FOM = $\mu\beta/M$, where β is the hyperpolarizability of the chromophore and M is the molecular mass).

We initially worked with a composite of 25% Lemke (2-(3-(2-(4-dialkylaminophenyl)vinyl)-5,5-dimethylcyclohex-2-enyliden-e)malononitrile) and 75% PMMA. This composite, described earlier,[24] had $T_g \sim 85$ °C. More recently, we obtained better results by using chromophores with a stronger acceptor, dicyanodihydrofurane (DCDHF).[25] The THz experimental results presented in this paper correspond to composites of 40% DCDHF-6-V/60% APC and 20% DCDHF-6-V/20% DCDHF-MOE-V/60% APC. These composites have $T_g \sim 97$ °C. They are better than the Lemke composite in both their EO and THz performance and in their stability. We did not observe a significant degradation of the THz performance of our EO polymers over a period of a couple of weeks.

The preparation of our materials has been described earlier.[25] Briefly, films are cast from solution onto an indium tin oxide (ITO) coated glass substrate. After solvent evaporation, the solid polymer film is pressed in a vacuum at $T_g + 70$ °C for 10−15 min. The thickness of the resulting film is controlled by appropriate polyimide spacers. We can make films with thicknesses controlled in the range of 50−350 μm, but mostly we worked with 70−130 μm thick layers.

Initially, the chromophores inside the polymer layer are oriented randomly. The medium is centrosymmetric, so the second-order nonlinear optical susceptibility is zero. However a nonzero $\chi^{(2)}$ is required for nonlinear interactions such as optical rectification and electrooptic sensing (discussed in detail in the coming sections). To impart a polar order to the film, high voltage is applied to the ITO electrodes and the sample is heated to the glass transition temperature of the composite allowing the chromophores to orient in the electric field. The sample is then cooled to room temperature with the external electric field still applied, to freeze in the orientation of the chromophores, resulting in a nonzero $\chi^{(2)}$ at room temperature without an external field.

Thermal vibrations tend to randomize the orientation of the chromophores. Therefore, the poling state of the chromophores degrades with time. The higher the T_g of the composite the more stable the nonlinearity. In the weak field approximation the electrooptic coefficient is directly proportional to the poling field,[26]

$$r_{33} = \frac{2N}{5}\left(\frac{\epsilon(n^2+2)^2}{3n^2(n^2+2\epsilon)}\right)^2 \beta_{zzz}\frac{\mu E_p}{kT} \qquad (1)$$

where N is the number density of chromophores, ϵ is the static dielectric constant, n is the material refractive index, β_{zzz} is the second order polarizability, μ is the molecular dipole moment, k is Boltzman's constant, T is the absolute temperature, and E_p is the poling field. Our experimental results indicate a linear dependence (Figure 2) of r_{33} on the poling field. The EO coefficient is also directly proportional to the dipole moment μ and hyperpolarizability β of the chromophores. In Figure 2, we can see that for the same poling field, the DCDHF-6-V chromophore has a larger EO coefficient than Lemke because the latter has a lower dipole moment and β.[25] For our typical poling field of 80−100 V/μm, the EO polymer composites have EO coefficients about 1 order of magnitude larger than that of ZnTe.

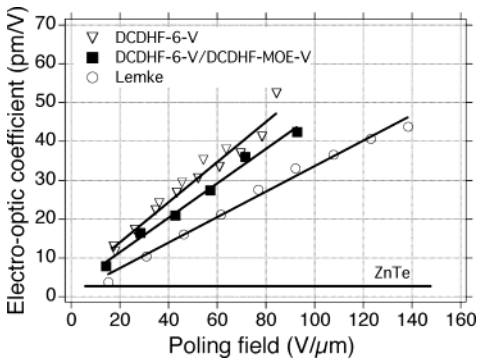

Figure 2. Electrooptic coefficient at 785 nm as a function of the poling field for composites with 40% Lemke, 40% DCDHF-6-V and 20% DCDHF-6-V/20% DCDHF-MOE-V mixed with 60% APC. Solid lines are a fit to the linear function. For comparison, the EO coefficient of ZnTe (4 pm/V at 800 nm) is also shown.

The plot in Figure 2 was obtained using EO polymer layers 70−130 μm thick. Thicker layers (>300 μm) have been prepared, but lower EO coefficients (about 20 pm/V) are obtained due to the inability to apply sufficiently high voltages. It is technically difficult to apply more than ~12 000 V in our current apparatus. However, there seem to be no physical limitations to the poling of polymers to achieve the same high EO coefficients (>50 pm/V) with thick layers.

THz Experiment

Optical rectification (OR)[27] is widely used to generate THz radiation in EO materials. In this scheme, short laser pulses (10−200 fs) pump the nonlinear medium. These pulses contain a range of frequencies. When these frequencies are present inside the nonlinear medium, difference frequency mixing results in the generation of broadband radiation in the THz regime.[28]

To test our materials, we used a standard THz generation and detection scheme (Figure 3). The laser beam from an amplified femtosecond laser (Spectra Physics SpitFire; 45 fs,

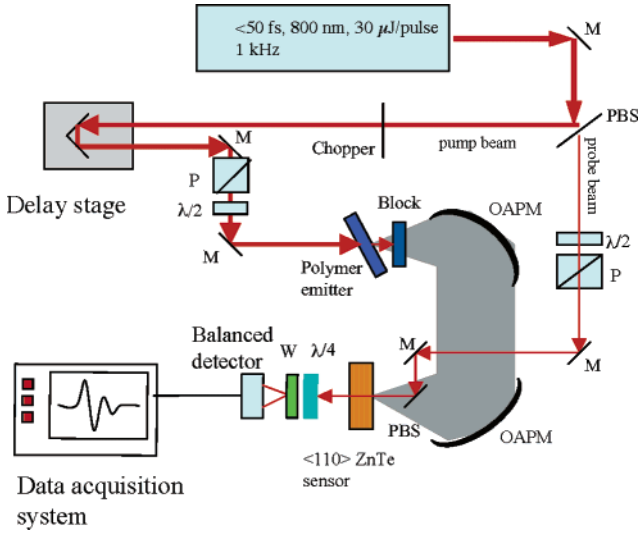

Figure 3. Experimental setup. P is a polarizer, W is a Wollaston prism, M is a mirror, PBS is a 5 μm pellicle beam splitter, OAPM is an off-axis parabolic mirror, $\lambda/2$ and $\lambda/4$ are half- and quarter-wave plates. The data acquisition system consists of a lock-in amplifier which acquires the signal from balanced photodiodes. A reference signal for the lock-in amplifier is obtained from a chopper operating at 300−1500 Hz.

30 μJ/pulse, 800 nm, 1 kHz) is split by a 5 μm pellicle beam splitter into pump and probe beams. The pump beam is incident on the polymer or crystal emitter which is located at the focus of the first off-axis parabolic mirror. The generated THz field is collimated and focused onto the ZnTe sensor by the pair of off-axis parabolic mirrors. A 5 mm thick high-density polyethylene disk or 10 mm polystyrene foam, which is transparent to the THz wave but absorbs the optical beam, is placed after the emitter to block the residual pump beam. The linear EO effect[29] is used to detect the THz wave. When a linearly polarized probe beam is incident on the detecting crystal without a THz field, its polarization is not altered. The balanced detector (2 photodiodes connected oppositely) shows no signal at this time; both channels give the same current with opposite polarity. The electric field from an incident THz wave changes the probe beam's polarization via the EO effect, which causes a different amount of light to reach each photodiode. This change is detected by a lock-in amplifier. The probe pulse duration (50 fs) is much smaller than the THz period (1 ps). Therefore, movement of the computer controlled delay stage changes the time delay between the pump and the probe pulses and allows the temporal dependence of the THz electric field to be sampled with the resolution of the probe pulse.

THz Generation via Optical Rectification with EO Polymers

In this section, we present a simple model of the THz field generated from a poled polymer layer and detected with a ZnTe crystal. The purpose of this model is to illuminate the general features of THz generation in poled polymers.

A poled polymer is in the material class ∞mm. Choosing the Z-axis parallel to the poling electric field, the nonlinear susceptibility tensor of the polymer (in the polymer frame) is

$$d_{ijk} = d_{il} = \begin{pmatrix} 0 & 0 & 0 & 0 & d_{15} & 0 \\ 0 & 0 & 0 & d_{15} & 0 & 0 \\ d_{31} & d_{31} & d_{33} & 0 & 0 & 0 \end{pmatrix} \qquad (2)$$

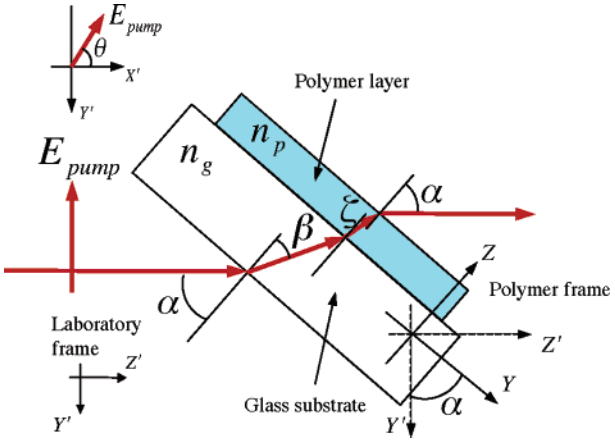

Figure 4. Optical pump beam incident on the polymer layer on the glass substrate, α is the angle of incidence, β and ζ are the pump beam propagation angles in the substrate and polymer layer, respectively. $X'Y'Z'$ is the laboratory frame, and XYZ is the polymer frame. n_g and n_p are the refractive indices of the glass substrate and polymer layer, respectively. The pump field in the $X'Y'$ plane of the laboratory frame is shown at the top of the figure.

In the laboratory frame, $X'Y'Z'$ (Figure 4), the incident pump beam propagating in the Z' direction has the components

$$E_{X'} = E_0 \cos\theta$$
$$E_{Y'} = -E_0 \sin\theta$$
$$E_{Z'} = 0 \qquad (3)$$

where E_0 is the pump field amplitude and θ is the angle between the X' axis and the pump beam polarization (the $X'Y'$ plane is shown at the top of Figure 4). After refraction at the air−glass and glass−polymer interfaces, the pump field has the components (in the polymer frame)

$$E_X = E_{X'} t_{sAG} t_{sGP} = E_o (t_{sAG} t_{sGP}) \cos\theta$$
$$E_Y = -E_{Y'} t_{pAG} t_{pGP} \cos\zeta = E_0 (t_{pAG} t_{pGP}) \sin\theta \sqrt{1 - \frac{\sin^2\alpha}{n_p^2}}$$
$$E_Z = E_{Y'} t_{pAG} t_{pGP} \sin\zeta = E_0 (t_{pAG} t_{pGP}) \sin\theta \frac{\sin\alpha}{n_p} \qquad (4)$$

where ζ is the angle of the pump beam propagation angle inside the polymer layer with refractive index n_p, and t_{sAG}, t_{pAG}, t_{sGP}, t_{pGP} are the Fresnel transmission coefficients for the s- and p-polarizations at the air−glass (AG) and glass−polymer (GP) interfaces, and α is the angle of incidence.

The nonlinear polarization induced inside the polymer will have the components,[27]

$$\begin{pmatrix} P_X \\ P_Y \\ P_X \end{pmatrix} = \begin{pmatrix} 0 & 0 & 0 & 0 & d_{15} & 0 \\ 0 & 0 & 0 & d_{15} & 0 & 0 \\ d_{31} & d_{31} & d_{33} & 0 & 0 & 0 \end{pmatrix} \begin{pmatrix} E_X E_X \\ E_Y E_Y \\ E_Z E_Z \\ 2E_Y E_Z \\ 2E_X E_Z \\ 2E_X E_Y \end{pmatrix} \qquad (5)$$

and can therefore be written as follows:

$$P_X(\theta,\alpha) = 2d_{15}E_XE_Z = 2d_{15}E_0{}^2(t_{pAG}t_{pGP}t_{sAG}t_{sGP})\sin\theta\cos\theta\frac{\sin\alpha}{n_p}$$

$$P_Y(\theta,\alpha) = 2d_{15}E_ZE_Y = 2d_{15}E_0{}^2(t_{pAG}t_{pGP})^2\sin^2\theta\frac{\sin\alpha\sqrt{n_p{}^2-\sin^2\alpha}}{n_p{}^2}$$

$$P_Z(\theta,\alpha) = d_{31}(E_X{}^2+E_Y{}^2)+d_{33}E_Z{}^2 = d_{31}E_0{}^2\left\{\cos^2\theta(t_{sAG}t_{sGP})^2+\sin^2\theta(t_{pAG}t_{pGP})^2\left(1-\frac{\sin^2\alpha}{n_p{}^2}\right)\right\}+ d_{33}E_0{}^2\sin^2\theta\,(t_{pAG}t_{pGP})^2\frac{\sin^2\alpha}{n_p{}^2} \quad (6)$$

Neglecting birefringence of the medium, we assume that the amplitude of the generated THz field is directly proportional to the induced nonlinear polarization, $E_{THz} \propto P_{NL}$. This simplified approach allows us to easily obtain the formula for the THz field and to model the system of an EO polymer emitter and a ZnTe detector. As will be shown in the next section, this model corresponds to the experimental results and gives the correct behavior for both the amplitude and the polarization of the THz field generated from a poled polymer. An exact model of THz generation from a poled polymer based on the solution of the nonlinear wave equation will be presented elsewhere.[30]

After refraction at the polymer−air interface, the THz electric field in the lab frame will have the components,

$$E_X{}'^{THz}(\theta,\alpha) = At_{sPA}P_X(\theta,\alpha),$$
$$E_Y{}'^{THz}(\theta,\alpha) = Bt_{pPA}\sqrt{P_Y{}^2(\theta,\alpha)+P_Z{}^2(\theta,\alpha)},$$
$$E_Z{}'^{THz}(\theta,\alpha) = 0 \quad (7)$$

where A and B are constants and t_{sPA} and t_{pPA} are the Fresnel coefficients at the polymer−air interface for s- and p-polarizations.

The transmitted THz electric field amplitude in the lab frame is given by

$$E^{THz}(\theta,\alpha) = \sqrt{(E_X{}^{THz}(\theta,\alpha))^2+(E_Y{}^{THz}(\theta,\alpha))^2+(E_Z{}^{THz}(\theta,\alpha))^2} \quad (8)$$

If we define the THz polarization angle γ as the angle between the THz electric field vector and the $-Y'$ axis in the lab frame, then

$$\sin\gamma(\theta,\alpha) = \frac{E_X{}^{THz}(\theta,\alpha)}{E^{THz}(\theta,\alpha)} = \frac{t_{sPA}AP_X(\theta,\alpha)}{\sqrt{(t_{sPA}AP_X(\theta,\alpha))^2+t_{pPA}{}^2B^2(P_Y{}^2(\theta,\alpha)+P_Z{}^2(\theta,\alpha))}} \quad (9)$$

THz detection with a ZnTe crystal has been studied in detail by Planken et al. They find that the signal intensity due to the linear EO effect in ZnTe is given by the expression[16]

$$I_{signal}(\theta,\alpha) = I_{probe}\frac{\omega n^3 r_{41}L}{2c}E_{THz}(\theta,\alpha)[\cos\gamma(\theta,\alpha)\sin 2\phi + 2\sin\gamma(\theta,\alpha)\cos 2\phi] \quad (10)$$

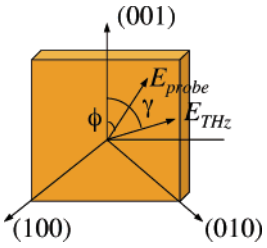

Figure 5. Detection geometry for a ⟨110⟩ ZnTe sensor. E_{probe} and E_{THz} are the probe and THz electric field vectors, respectively, and ϕ and γ are their respective polarization angles in the crystal surface plane.

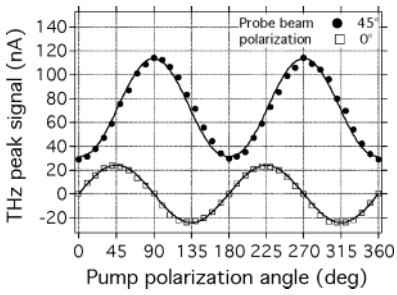

Figure 6. Angular dependence of the THz signal as a function of the pump polarization angle for two probe beam angles. Solid lines are calculated by eq 10.

where I_{probe} is the probe beam intensity, ω is the optical frequency, r_{41} is the EO coefficient of ZnTe at the probe wavelength, n is the refractive index of ZnTe at the probe wavelength, L is the crystal thickness, ϕ is the angle between the probe beam polarization and the (001) direction of the crystal, and γ is the angle between THz field polarization and the (001) direction of the crystal in the crystal surface plane (Figure 5).

Using the angular dependence of the THz amplitude $E_{THz}(\theta,\alpha)$ (eq 8) and the THz polarization angle $\gamma(\theta,\alpha)$ (eq 9) in eq 10 gives the dependence of the detected signal as a function of the pump polarization angle θ for any probe beam angle ϕ.

THz Performance of Polymers

To confirm our model of THz generation in a poled polymer via optical rectification, we experimentally determined the angular dependence of the detected THz signal as a function of the pump beam polarization for probe beam polarizations of 45 and 0°. The data are shown in Figure 6 along with a fit to eq 10. The data were obtained by fixing the delay stage at the position corresponding to the maximum of the THz field while rotating the pump beam polarization. The angle of incidence was near 56° which corresponds to the Brewster angle for glass. The maximum amplitude of the generated THz field for the 45° polarized probe beam corresponds to p-polarization (θ = 90°) of the pump beam just as for second harmonic generation in poled polymers.

Figure 7 shows a direct comparison of a ZnTe crystal and polymer emitters.

Comparing the peak to peak detected signal, we see that the THz field emitted from the 80 μm EO polymer film is equal to that emitted from the 1 mm ZnTe crystal. Signal-to-noise (SNR) in this experiment is about 100. Unfortunately, the damage threshold of our current materials is lower than that of the crystals. For this reason we cannot illuminate the emitter with the whole power available from the laser system or focus the pump beam tightly, resulting in a lower SNR. The pump power used in this comparison was 3 mW in ~0.5 mm spot.

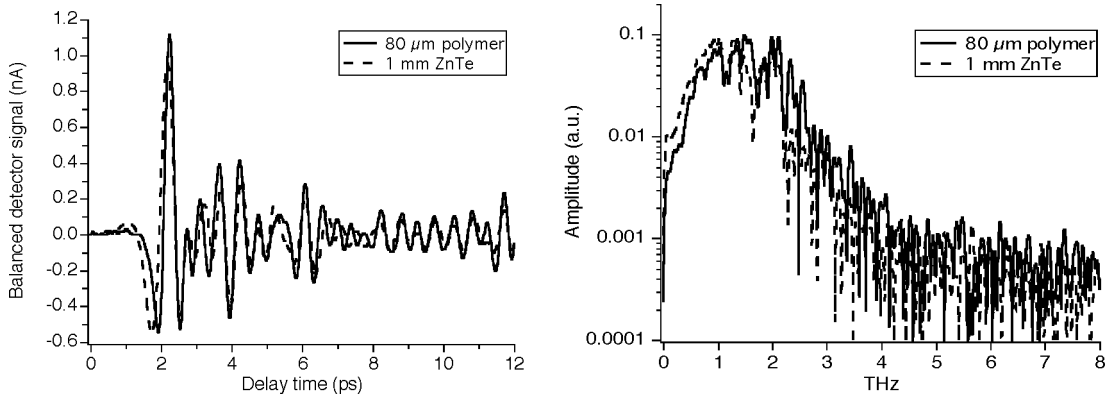

Figure 7. Comparison of the THz field emitted from a 1 mm ZnTe crystal and an 80 μm polymer layer (40%DCDHF-6-V/60%APC). The EO coefficient of the polymer is 47 $\pm$ 2 pm/V. A 2 mm thick ZnTe sensor is used in both cases. Temporal traces (left) and corresponding Fourier transforms (right) are shown.

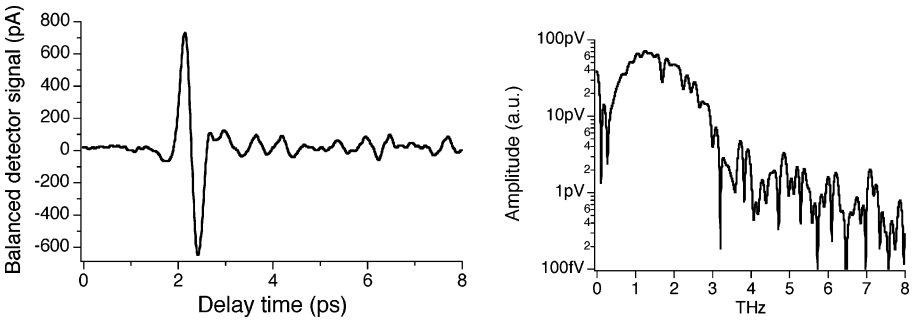

Figure 8. THz signal from a pair of EO polymers used as both an emitter and a sensor of THz radiation (left). A 130 μm single layer of 20%DCDHF-6-V/20%DCDHF-MOE-V/60%APC with an EO coefficient of 40 pm/V was used. THz spectrum of this pulse (right). This experiment is performed in the open air. Several strong absorptions due to water vapor are evident.

It is necessary to specify the conditions of this comparison. The ZnTe sensor orientation was kept the same for both polymer and ZnTe emitters. The probe beam polarization was perpendicular to the plane of incidence (POI) and parallel to the *z*-axis of the ZnTe sensor so that $\phi = 0°$ in eq 10. This means that the maximum signal is obtained with the THz field polarization is parallel to the POI for which $\gamma = 90°$ in eq 10. This kind of THz field is generated from the polymer layer when the pump beam polarization is parallel to the POI (p-polarized for the polymer emitter). In contrast, to get the same polarization of THz field from the ZnTe emitter, the pump beam must be polarized perpendicular to the POI and the crystal *z*-axis must be parallel to the POI, so the angle between the pump beam polarization and the emitter *z*-axis is 90°.[15] This combination of the polarization of the pump beam and the orientation of the emitter gives the maximum THz signal when the ZnTe sensor is oriented as described above. About 15% more THz power can be obtained from the crystal when the angle between *z*-axis of crystal and the pump beam is 55°.[15] However, in this case the THz field polarization is no longer parallel to the POI, requiring a reorientation of the ZnTe sensor. We elected to retain a fixed and common sensor orientation and detection optics alignment for comparison of emitters.

Previously, Nahata et al.[21] reported a 4 times smaller THz amplitude from a 16 μm thick EO polymer compared to that from a 1 mm thick crystal of $LiNbO_3$. Carrig[31] reported that DAST is 11 times better that $LiNbO_3$ for similar thicknesses. Han[32] reported the THz amplitude from 100 μm of DAST to be 6 times larger than that from 30 μm of ZnTe. Thus, we estimate that 1 mm of ZnTe should be about 20 times better than the 16 μm film of Nahata's group. Also, Carey et al.[20] demonstrated that 200 μm of the organic crystal MBANP gives a 2.5 times better THz signal than 500 μm of ZnTe. This means that, at 800 nm, 80 μm of our EO polymer gives about the same THz amplitude as obtained from 200 μm of MBANP or 500 μm of DAST. For all these comparisons, the dependence of the generated THz field amplitude vs the emitter thickness is assumed to be linear.

Figure 8 shows our experimental result of THz emission and detection using only a poled polymer. For this experiment, a poling field of ~80 V/μm was used to pole two individual 130 μm films, resulting in an EO coefficient of 40 pm/V for each. One film was used as the emitter and other was used as the sensor. This experiment was performed in the open air with 50 fs ($\Delta\lambda \sim 30$ nm) pulses at 800 nm. A signal-to-noise ratio of about 100 was observed. This low SNR is a result of low pump power incident on the emitter.

Coherence Length and THz Frequency Response

In a nonlinear process, pump waves interact inside a nonlinear medium resulting in the appearance of new waves. For example, in second harmonic generation, two fields of a single frequency produce a field of a doubled frequency. In these interactions, energy is transferred from one field to others. This energy interchange is efficient if the velocities of the waves in the nonlinear medium are matched. Because of material dispersion, this "phase matching" only occurs over a narrow range of frequencies. When two waves of different frequencies propagate in a medium, the difference in their velocities will be determined by the difference in their refractive indices at these frequencies. When generating THz radiation via OR, the appropriate velocities are the optical group velocity associated with the short pump pulse and the THz phase velocity associated with the generated THz wave.

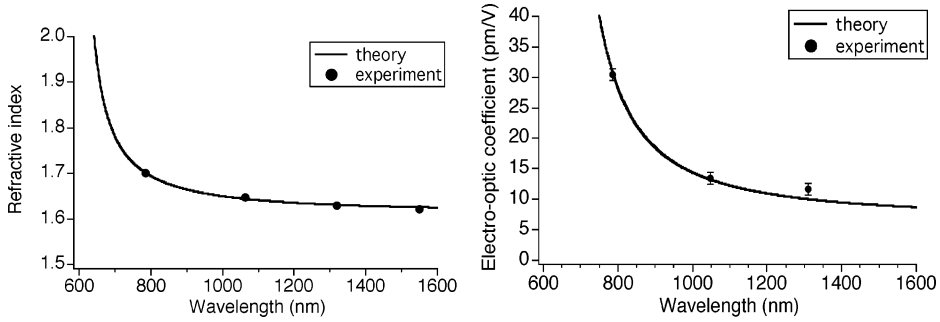

Figure 9. Left: Optical dispersion of 40%DCDHF-6-V/60%APC. Solid line is a fit of a Sellmeier dispersion formula[12] to the experimental data (solid circles) with $\lambda_{abs} = 600$ nm, $A = 2.3951$, and $B = 0.2072$. Right: dispersion of the EO coefficient calculated with eq 17 fitted to the experimental data with $D = 3.1$.

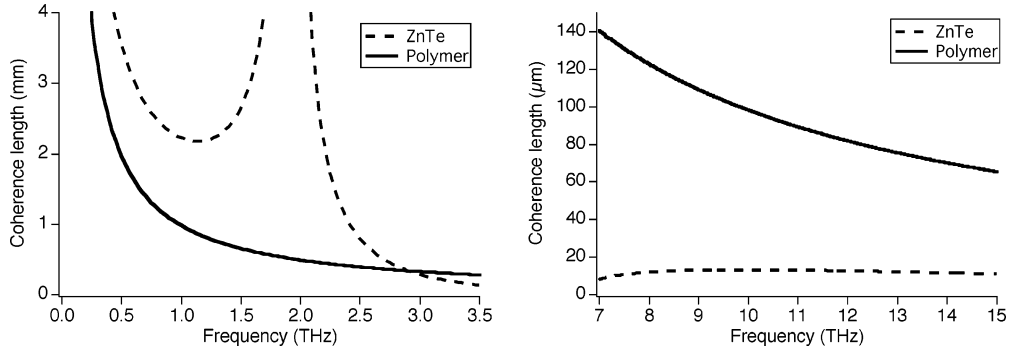

Figure 10. Left: Coherence length in ZnTe and a polymer composite of 40% DCDHF-6-V/40% APC calculated by eq 11 with our experimental index data. Right: The projected coherence length of the same materials in the range 7−15 THz.

In general, the coherence length is inversely proportional to the difference of the optical group index and the THz refractive index. Taking into account material dispersion, Nahata[33] finds that the coherence length for OR is

$$L_c = \frac{\pi c}{\Omega_{THz}\left|n_{opt} - \lambda_{opt}\left(\frac{dn_{opt}}{d\lambda}\right)_{\lambda opt} - n_{THz}\right|} \qquad (11)$$

where n_{opt} and n_{THz} are the optical and THz refractive indices of the material respectively, Ω_{THz} is the THz angular frequency, λ_{opt} is the wavelength of the pump beam, and c is the speed of light.

In OR, the amplitude of the generated THz wave increases with the thickness of the nonlinear medium. The linear EO effect is also directly proportional to the thickness of the nonlinear medium. Therefore, to obtain greater THz power from an emitter as well as high sensitivity and signal-to-noise ratio in THz EO detectors, it is important to increase the thickness of both the emitter and detector as much as possible. However, if the coherence length is small, the optical group velocity and the THz phase velocity will only be matched for a limited range of THz frequencies. Therefore, materials with shorter coherence lengths will have narrower frequency responses.

The optical and THz refractive index of ZnTe, which is widely used in THz experiments, is well-known.[33] The dispersion of the 40%DCDHF-6-V/60%APC composite is presented in Figure 9 (left) by fitting of the Sellmeier dispersion formula

$$n^2 = A + \frac{B\lambda^2}{\lambda^2 - \lambda_{abs}^2} \qquad (12)$$

to our experimental data (solid circles). For $\lambda_{abs} = 600$ nm the best fit is obtained with $A = 2.3951$, $B = 0.2072$. The dispersion in our material is calculated to be $-0.45\ \mu m^{-1}$ at 800 nm. We measured the THz refractive index to be 1.9 in the range 0.5−3.5 THz by transmitting a THz pulse through a 130 μm thick layer of DCDHF-6-V/APC.

Comparing the coherence length of ZnTe to that of our polymers, we note the following (Figure 10 left): at ∼2 THz in ZnTe the group velocity of the optical pulse is matched with the THz phase velocity, resulting in a sharp resonance. In the low frequency range, the crystal is definitely better than the polymer. However, as the THz frequency increases, the coherence length in polymers should become larger than that of the crystal (Figure 10, right). However, additional measurements are necessary to experimentally support this prediction since our measurements on the polymer only covered the 0.5−3.5 THz region.

Previously, Nahata et al.[21] reported the coherence length for EO polymer to be 1.9 mm at 0.5 THz and 0.95 mm at 1 THz, which is about 20 times larger than that of $LiNbO_3$. A wideband response up to 33 THz has been experimentally demonstrated with this kind of EO polymer sensor.[23]

The frequency response of an EO sensor has been studied in detail.[18,34,35] The detected THz signal is represented as a product of three frequency dependent terms:[34] the first term describes the frequency limitations of the light source, which depend on the pulse duration of pump and probe beams, the second describes the EO dispersion of the emitter and sensor, and the third one involves the group velocity mismatch (GVM) between optical and THz pulse as discussed above. These three terms act as filters affecting the frequency response of the whole THz system.

The goal of this section is to compare nonlinear media only; therefore, we will not take into consideration the limitations of

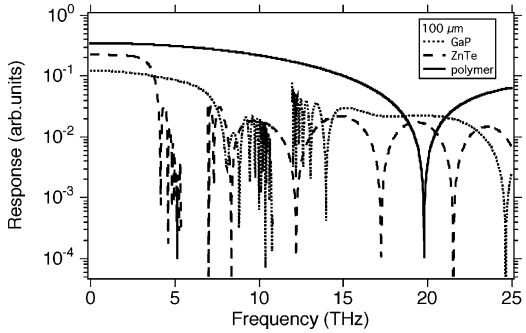

Figure 11. Calculated frequency response of 100 μm thick ZnTe, GaP, and EO polymer sensors from eq 12 for 800 nm for both ZnTe and EO polymers and 835 nm for GaP. $C = -0.07$ and -0.47 and $\gamma = 3.01$ and 4.3 cm^{-1} for ZnTe and GaP respectively.[35] The polymer and ZnTe were simulated at 800 nm and GaP at 835 nm. The group indices of the polymer, ZnTe, and GaP are 2.05, 3.24 and 3.56, respectively. The THz refractive index was calculated from eq 4 in ref 33 for ZnTe and from ref 38 for GaP.

the laser source, so the response function can be presented as[3]

$$R(\Omega) = r_{\mathrm{EO}}(\Omega)G(\Omega) \tag{13}$$

where $r_{EO}(\Omega)$ is the frequency dependent EO coefficient and $G(\Omega)$[18] is the GVM factor

$$G(\Omega) = \frac{T(\Omega)}{\delta(\Omega)}\int_0^{\delta(\Omega)} \mathrm{e}^{i2\pi\Omega t}\,\mathrm{d}t = \frac{T(\Omega)(\mathrm{e}^{i2\pi\Omega\delta(\Omega)} - 1)}{i2\pi\Omega\delta(\Omega)} \tag{14}$$

with the Fresnel transmission coefficient for THz waves $T(\Omega)$

$$T(\Omega) = \frac{2}{1 + n_{\mathrm{THz}}(\Omega)} \tag{15}$$

and

$$\delta(\Omega) = \frac{L}{c}(n_{\mathrm{g}}(\lambda_0) - n_{\mathrm{THz}}(\Omega)) \tag{16}$$

is the GVM time,[18] where $n_{\mathrm{g}}(\lambda_0)$ is the material group index at the probe wavelength λ_0, $n_{\mathrm{THz}}(\Omega)$ is the THz refractive index, L is the EO sensor thickness, and c is the speed of light.

By applying time dependent perturbation theory in the two-level model approximation,[36] the dispersion of the EO coefficient in poled polymers can be written as

$$r_{33}(\lambda) = D\left(\frac{n^2(\lambda) + 2}{n^2(\lambda)}\right)^2 \frac{\lambda^2(3\lambda^2 - {\lambda_{\mathrm{abs}}}^2)}{(\lambda^2 - {\lambda_{\mathrm{abs}}}^2)^2} \tag{17}$$

where D is a constant, λ_{abs} is the wavelength of the absorption maximum, and λ is the optical wavelength. Figure 9 (right) shows the fit of this equation to the experimental measurements for our material. Being purely electronic, the nonlinearity of EO polymers is expected to remain constant in the mid- and far-infrared frequency ranges.

In contrast to EO polymers, the nonlinearity in crystals is mostly ionic.[18] The frequency dependent $r_{EO}(\Omega)$ is modeled for GaP and ZnTe as[35]

$$r_{\mathrm{EO}}(\Omega) = r_{\mathrm{e}}\left(1 + \frac{C(\hbar\Omega_{\mathrm{TO}})^2}{(\hbar\Omega_{\mathrm{TO}})^2 - (\hbar\Omega)^2 + i\hbar\Omega\gamma}\right) \tag{18}$$

where r_{e}, C, and γ are constants and Ω_{TO} is the transverse-optical phonon frequency. Crystals are characterized by phonons associated with lattice vibrations. For example, there are phonon absorption bands in ZnTe at 5.3 THz, in InP at 9 THz, and in GaP at 11 THz.[18,35]

Figure 11 shows the comparison of the frequency response of 100 μm thick ZnTe, GaP, and EO polymer sensors calculated by eq 13. Both the EO dispersion (eqs 17 and 18) and the GVM (eq 14) affect the response. Because of resonances, many gaps can be seen in both the ZnTe and GaP responses. These spectral distortions are observed experimentally.[35,37] In contrast, since poled polymers are amorphous materials without phonon bands, their EO coefficient is frequency independent in the mid- and far-infrared range and a flatter frequency response at least up to 20 THz is anticipated. An almost flat response over 20 THz has been observed experimentally in a poled polymer THz sensor.[23]

A large coherence length due to low dispersion and the absence of phonons together with high EO coefficients make EO polymers attractive materials for THz experiments.

Conclusion

We have reported an experimental study of THz generation and detection with poled polymers. We have developed a technique to obtain poled polymer layers with thicknesses in the range of 50−350 μm. These polymers are more efficient THz emitters and detectors than the standard ZnTe crystal. Direct comparison shows that the THz field emitted from an 80 μm thick poled polymer is equal to that emitted from a 1 mm thick ZnTe crystal.

In comparison to crystals, EO polymers have two distinct advantages, higher EO coefficients and larger coherence lengths at high frequencies. Both these factors are important for THz applications, especially wideband applications, because the thickness of emitters and detectors should be large to provide a high sensitivity and signal-to-noise ratio without limiting the frequency response. Additionally, polymers are amorphous materials and therefore they do not have phonon absorption bands.

EO polymers are versatile, permitting various chromophores and polymer matrices to be employed to fit specific requirements such as peak absorption and material refractive index. In addition, EO polymer composites are easy to prepare and cheap compared to crystals.

However, EO polymers have some disadvantages. First, thermal vibrations tend to randomize the poled order of chromophores decreasing the nonlinear properties of the medium over time. However, our current EO polymers can be used for at least a couple of weeks without significant degradation of EO properties if stored at room temperature. Higher T_{g} EO polymers with larger EO coefficients are being developed.[39] These materials exhibit no appreciable degradation of their EO coefficient over thousands of hours when stored at 85 °C. Another disadvantage of EO polymers is that the thickness of a highly poled polymer layer is limited to a few hundred micrometers. This is because an extremely high voltage needs to be applied to a thick layer in order to achieve a high poling field. However, as discussed above, the wide frequency response requires thin and efficient emitters and sensors, so this limitation may not be significant for wideband applications. Also, EO polymers, when illuminated near their absorption maximum, have a low damage threshold compared to crystals. This does not allow high pump powers and limits our SNR, currently.

We also developed a theoretical model of THz generation from a poled polymer via optical rectification and verified this model experimentally in a system using a polymer emitter and

a ZnTe sensor. This model allows the adjustment of the orientation of both the emitter and detector for the best THz performance for a given combination of pump and probe beam polarizations.

In this study we did not yet demonstrate a wideband THz spectrum. In the future we plan to perform the THz experiments with polymers in a dry environment with shorter laser pulses to demonstrate a wideband spectral response. We also plan to study the THz absorption in our materials.

Acknowledgment. The authors thank Robert Twieg and Meng He from Kent State University for providing the DCDHF chromophores and Warren Herman from the Laboratory for Physical Sciences for measuring the optical refractive indices of our EO polymer films. This work is supported by the National Science Foundation (ECS-0139457).

References and Notes

(1) Mittleman, D.; Jacobsen, R. H.; Nuss, M. *IEEE J. Sel. Topics Quantum Elect.* **1996**, *2*, 679.
(2) Fitzgerald, A. J.; Berry, E.; Zinovev, N. N.; Walker, G. C.; Smith, M. A.; Chamberlain, J. M. *Phys. Med. Biol.* **2002**, *47*, R67.
(3) Smye, S. W.; Chamberlain, J. M.; Fitzgerald, A. J.; Berry, E. *Phys. Med. Biol.* **2001**, *46*, R101.
(4) Mittleman, D. M.; Gupta, M.; Neelamani, R.; Baraniuk, R. G.; Rudd, J. V.; Koch, M. *Appl. Phys. B: Laser Opt.* **1999**, *68*, 1085.
(5) Hu, B. B.; Nuss, M. C. *Opt. Lett.* **1995**, *20*, 1716.
(6) Cheville, R. A.; Grischkowsky, D. *Opt. Lett.* **1995**, *20*, 1646.
(7) Cheville, R. A.; Grischkowsky, D. *Appl. Phys. Lett.* **1995**, *67*, 1960.
(8) Cheville, R. A.; McGowan, R. W.; Grischkowsky, D. *IEEE Trans. Antenn. Propag.* **1997**, *45*, 1518.
(9) Krishnamurthy, S.; Reiten, M. T.; Harmon, S. A.; Cheville, R. A. *Appl. Phys. Lett.* **2001**, *79*, 875.
(10) Nuss, M. C.; Orenstein, J. Terahertz time-domain spectroscopy. In *Millimeter and Sub-millimeter Wave Spectroscopy in Solids*; Grüner, G., Ed.; Springer: Berlin, 1998; Vol. 74; p 7.
(11) Grischkowsky, D.; Keiding, S.; van Exter, M.; Fattinger, C. *J. Opt. Soc. Am. B* **1990**, *7*, 2006.
(12) van Exter, M.; Fattinger, C.; Grischkowsky, D. *Opt. Lett.* **1989**, *14*, 1128.
(13) Duvillaret, L.; Garet, F.; Coutaz, J. L. *IEEE J. Sel. Topics Quantum Elect.* **1996**, *2*, 739.
(14) Han, P.; Zhang, X. C. *Meas. Sci. Technol.* **2001**, *12*, 1747.
(15) Chen, Q.; Tani, M.; Jiang, Z.; Zhang, X. C. *J. Opt. Soc. Am. B* **2001**, *18*, 823.
(16) Planken, P. C. M.; Nienhuys, H.-K.; Bakker, H. J.; Wenckebach, T. *J. Opt. Soc. Am. B* **2001**, *18*, 313.
(17) Wu, Q.; Zhang, X.-C. *IEEE J. Sel. Topics Quantum Elect.* **1996**, *2*, 693.
(18) Wu, Q.; Zhang, X.-C. *Appl. Phys. Lett.* **1997**, *70*, 1784.
(19) Pan, F.; Knöpfle, G.; Bosshard, C.; Follonier, S.; Spreiter, R.; Wong, M. S.; Günter, P. *Appl. Phys. Lett.* **1996**, *69*, 13.
(20) Carey, J. J.; Bailey, R. T.; Pugh, D.; Sherwood, J. N.; Cruickshank, F. R.; Wynne, K. *Appl. Phys. Lett.* **2002**, *81*, 4335.
(21) Nahata, A.; Auston, D.; Wu, C.; Yardley, J. T. *Appl. Phys. Lett.* **1995**, *67*, 1358.
(22) Nahata, A. *Opt. Lett.* **2001**, *26*, 385.
(23) Cao, H.; Heinz, T. F.; Nahata, A. *Opt. Lett.* **2002**, *27*, 775.
(24) Sinyukov, A. M.; Hayden, L. M. *Opt. Lett.* **2002**, *27*, 55.
(25) Hayden, L. M.; Sinyukov, A. M.; Leahy, M.; R.; French, J.; Lindahl, P.; Herman, W. N.; Twieg, R. J.; Meng, H. *J. Polym. Sci. B* **2003**, *41*, 2492.
(26) Bosshard, C. S.; K.; Pretre, Ph; Hulliger, J.; Florsheimer, M.; Kaatz, P.; Gunter, P *Organic Nonlinear Optical Materials*; Gordon and Breach Science Publishers SA: Basel, Switzerland, 1995; Vol. 1.
(27) Boyd, R. W. *Nonlinear Opt.*; Academic Press: San Diego, CA, 1992.
(28) Zhang, X.-C.; Jin, Y.; Ma, X. F. *Appl. Phys. Lett.* **1992**, *61*, 2764.
(29) Yariv, A. *Optical electronics*, 4th ed.; Saunders College Pub: Philadelphia, PA, 1991.
(30) Sinyukov, A. M.; Hayden, L. M. Unpublished work.
(31) Carrig, T. J.; Rodriguez, G.; Clement, T. S.; Taylor, A. J.; Stewart, K. R. *Appl. Phys. Lett.* **1995**, *66*, 121.
(32) Han, P. Y.; Tani, M.; Pan, F.; Zhang, X.-C. *Opt. Lett.* **2000**, *25*, 675.
(33) Nahata, A.; Weling, A.; Heinz, T. F. *Appl. Phys. Lett.* **1996**, *69*, 2321.
(34) Gallot, G.; Grischkowsky, D. *J. Opt. Soc. Am. B* **1999**, *16*, 1204.
(35) Leitenstorfer, A.; Hunschek, S.; Shah, J.; Nuss, M. C.; Knox, W. H. *Appl. Phys. Lett.* **1999**, *74*, 1516.
(36) Wortmann, R.; Poga, C.; Twieg, R. J.; Geletneky, C.; Moylan, C. R.; Lundquist, P. M.; DeVoe, R. G.; Cotts, P. M.; Horn, H.; Rice, J. E.; Burland, D. M. *J. Chem. Phys.* **1996**, *105*, 10637.
(37) Han, P. Y.; Zhang, X.-C. *Appl. Phys. Lett.* **1998**, *73*, 3049.
(38) Palik, E. D. *Handbook of Optical Constants of Solids*; Academic Press: Boston, MA, 1991.
(39) Ma, H.; Liu, S.; Luo, J.; Suresh, S.; Liu, L.; Kang, S. H.; Haller, M.; Sassa, T.; Dalton, L. R.; Jen, A. K. Y. *Adv. Funct. Mater.* **2002**, *12*, 565.